Real-Time Spatial Estimates of Snow-Water Equivalent (SWE)

Sierra Nevada Mountains, California

February 16, 2025

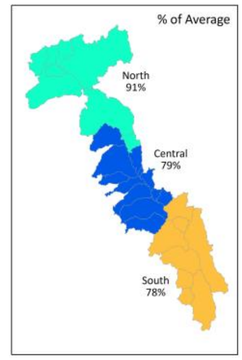

Team: Noah Molotch[1,2], Leanne Lestak[1], Emma Tyrrell[1] and Kehan Yang[1]
[1]Institute of Arctic and Alpine Research, University of Colorado Boulder
[2] Jet Propulsion Laboratory, California Institute of Technology
Contact: Leanne.Lestak@colorado.edu

Summary of current conditions

This year we've added the Trinity basin to our model runs. The regional summary map above shows the mean SWE above 5000' elevation for three major regions of the Sierra Nevada, percent of average is calculated from a long-term average of 2001-2021. Figure 2 contains comparison maps of CU SWE versus ASO SWE. Detailed SWE maps (in JPG format) and summaries of SWE (in Excel format) by individual basin and elevation band accompany the report and are publicly available on our website **here**.

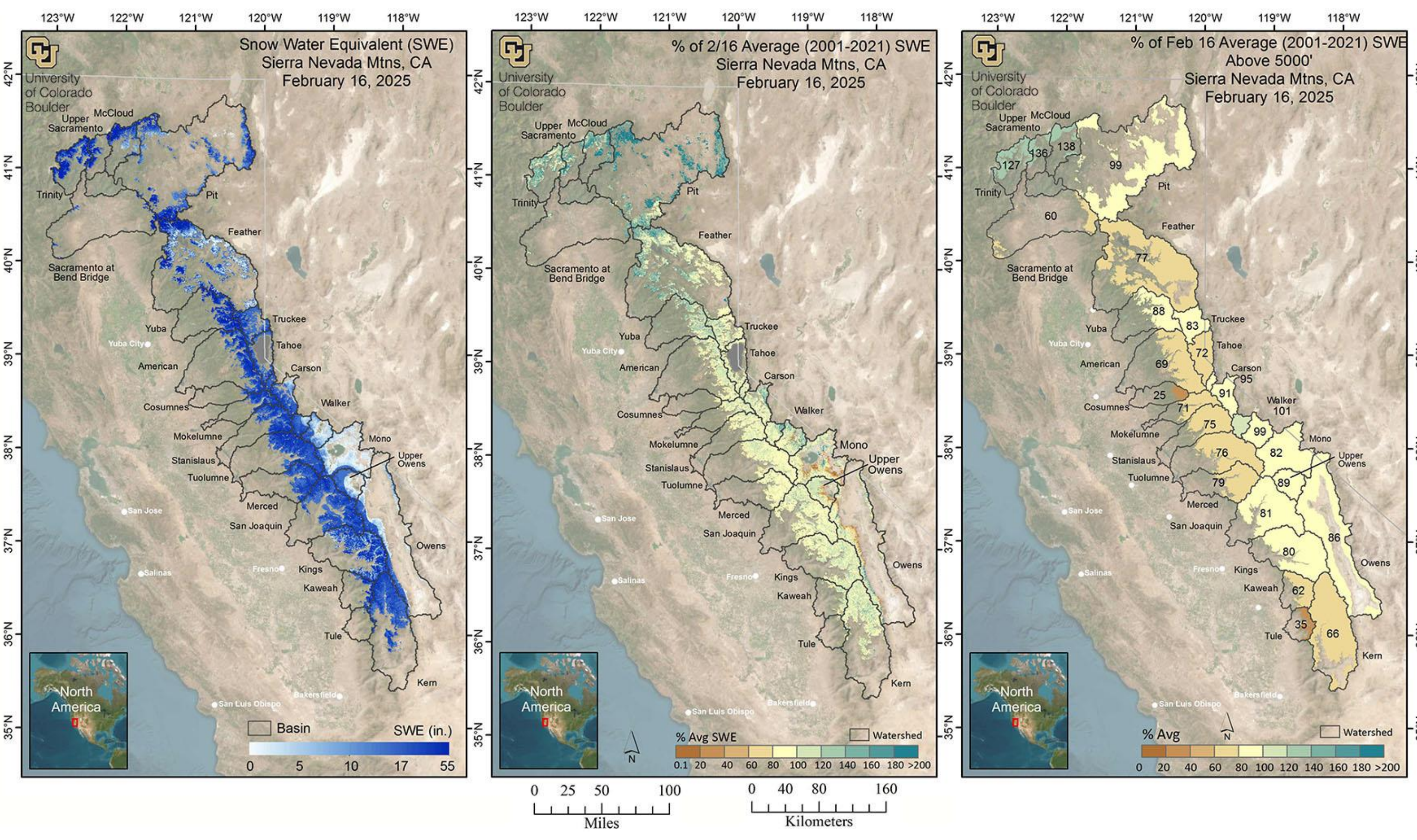

Figure 1. Estimated SWE and % of Average SWE across the Sierra Nevada. SWE amounts (left), and percent of average (2001-2021) SWE for the Sierra Nevada, calculated for each pixel (middle) and basin-wide (right). Basin-wide percent of average is calculated across all model pixels >5000' elevation.

Location of Reports and Excel Format Tables

https://github.com/CU-Mountain-Hydrology/SierraNevada

About this report

This is an experimental research product that provides near-real-time estimates of snow-water equivalent (SWE) at a spatial resolution of 500 m for the Sierra Nevada in California from mid-winter through the melt season. The report is typically released within a week of the date of data acquisition at the top of the report. A similar report covering the entire Western United States is available and is distributed to water managers across the western U.S. Note that SWE estimates in the northern basins may be low given recent and persistent cloud cover. See the forthcoming March 1 report which will contain cloud-free imagery.

The spatial SWE-fusion analysis method for the Sierra Nevada uses the following data as inputs:

- In-situ SWE from all operational CA and NV snow pillow sensor sites and CoCoRaHS SWE values when available and applicable
- Fractional snow-covered area (fSCA) data from recent cloud-free satellite images or model
- Physiographic information (elevation, latitude, upwind mountain barriers, slope, etc.)
- Historical daily SWE patterns (1985-2021) retrospectively generated using historical fSCA data and an energy-balance model that back-calculates SWE given the fSCA time-series and meltout date for each pixel.
- Satellite-observed daily mean fractional snow-covered area (DMFSCA)

For more details on the estimation method see the *Methods* section below. Please be sure to read the *Data Issues / Caveats* section for a discussion of persistent challenges or uncertainties of the SWE product.

Data availability for this report

There are a total of 134 snow pillow sites in the Sierra Nevada network that are used by the SWE-fusion model and when applicable there are typically 10-20 CoCoRaHS measurements that can be used. Sites that are recording SWE, offline sites, sites recording zero, and CoCoRaHS measurements are shown in Figure 6, on the left map (shown in black, red, yellow, and green respectively).

The value of spatially explicit estimates of SWE

Snowmelt makes up the large majority (~60-85%) of the annual streamflow in the Sierra Nevada. The spatial distribution of snow-water equivalent (SWE) across the landscape is complex. While broad aspects of this spatial pattern (e.g., more SWE at higher elevations and on north-facing exposures) are fairly consistent, the details vary a lot from year to year, influencing the magnitude and timing of snowmelt-driven runoff.

SWE is operationally monitored at over a hundred and thirty snow pillow sensor sites spread across the Sierra Nevada, providing a critical first-order snapshot of conditions, and the basis for runoff forecasts from the CA DWR, NRCS, and NOAA. However, conditions at snow pillow sites (e.g., percent of normal SWE) may not be representative of conditions in the large areas between these point measurements, and at elevations above and below the range of the sensor sites. The spatial snow analysis creates a detailed picture of the spatial pattern of SWE using snow sensors, satellite, and other data, extending beyond the snow sensor sites to unmonitored areas.

Interpreting the spatial SWE estimates in the context of snow pillows

The spatial product estimates SWE for every pixel where the fSCA product identifies snow-cover. Comparatively, snow sensor samples 8-20 points per basin within a narrower elevation range. Thus, the basin-wide percent of average from the spatial SWE estimates is not directly comparable with the snow sensor basin-wide percent of average. A better comparison might be made with the % of average in the elevation bands (Table 2) that contain snow sensor sites.

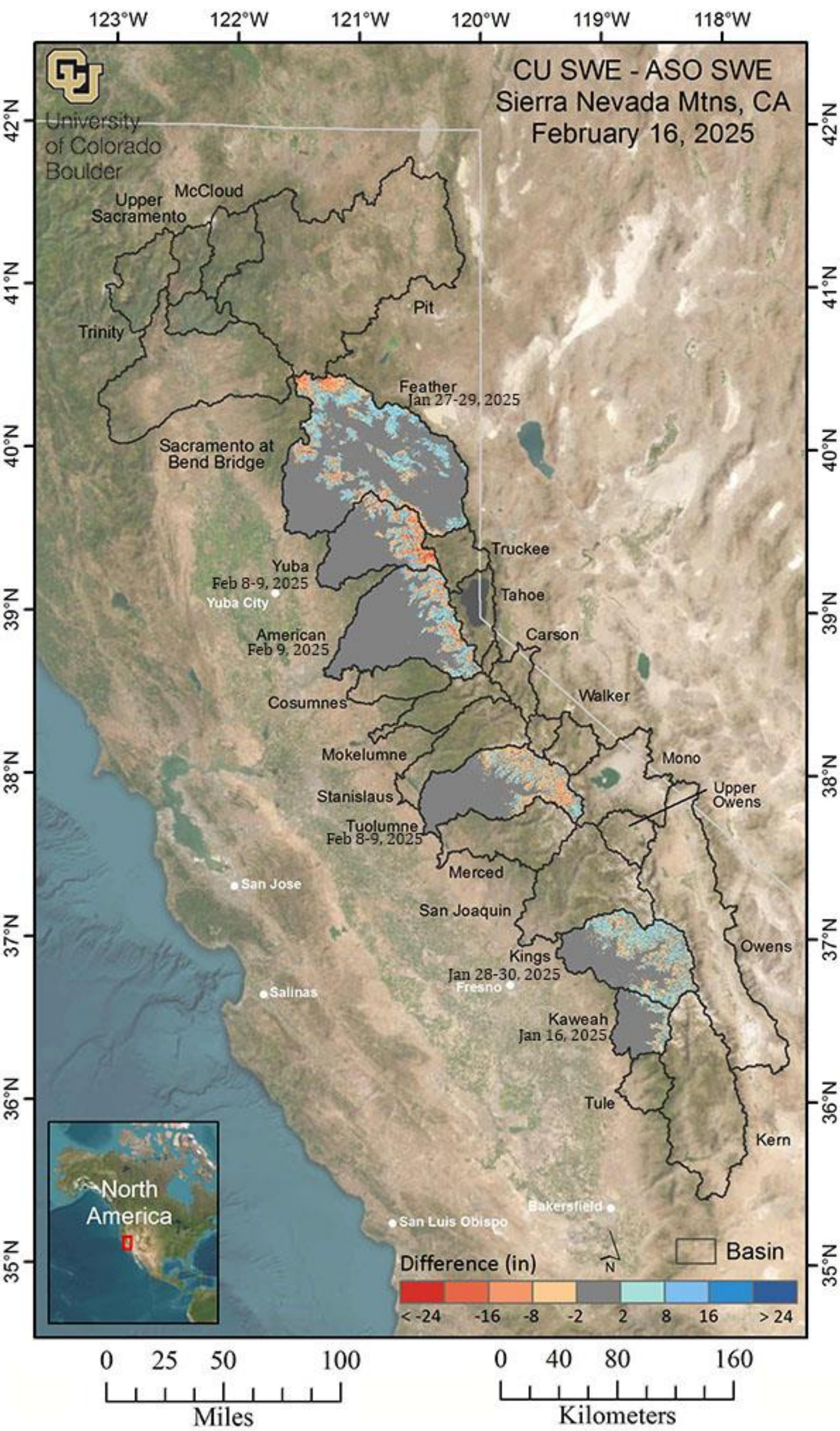

Figure 2. Comparison to ASO, Sierra Nevada. The difference in SWE amounts between the CU SWE-fusion model runs and Airborne Snow Observatories (ASO) lidar-derived SWE are shown for available basins flown this year. The date referenced to each basin, corresponds to the most recent ASO flight date where data has been released and is then compared to the CU SWE-fusion model run is that closest to the ASO flight date. Red colors show where CU SWE is lower than ASO SWE and blue colors show where CU SWE is higher than ASO SWE. This map will be updated as new ASO data becomes available. ASO data from current and sometimes past years are used to bias-correct our model data.

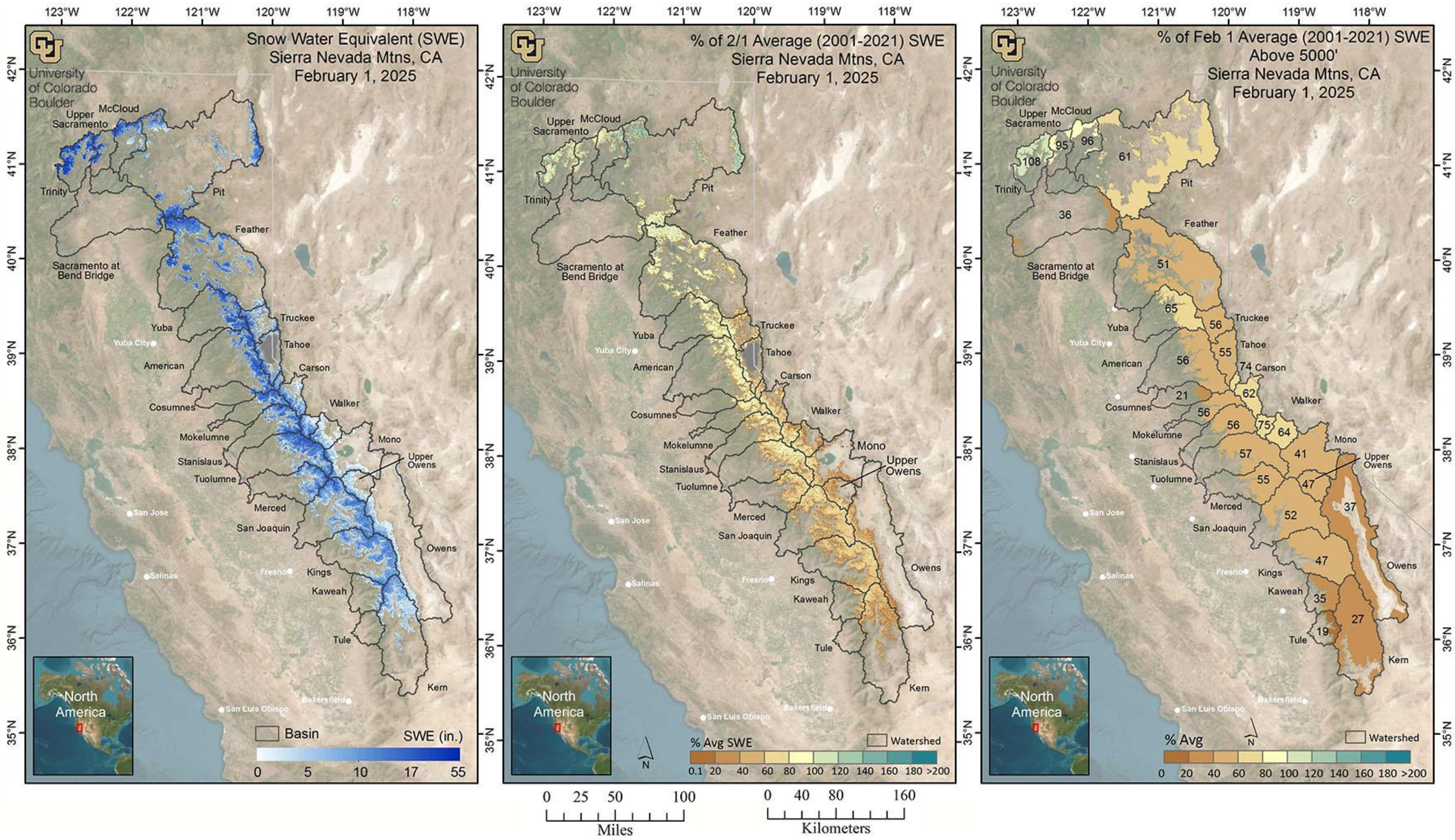

Figure 3. Estimated SWE and % of Average SWE across the Sierra Nevada. SWE amounts (left), and percent of average (2001-2021) SWE for the Sierra Nevada, calculated for each pixel (middle) and basin-wide (right). Basin-wide percent of average is calculated across all model pixels >5000' elevation for the previous report.

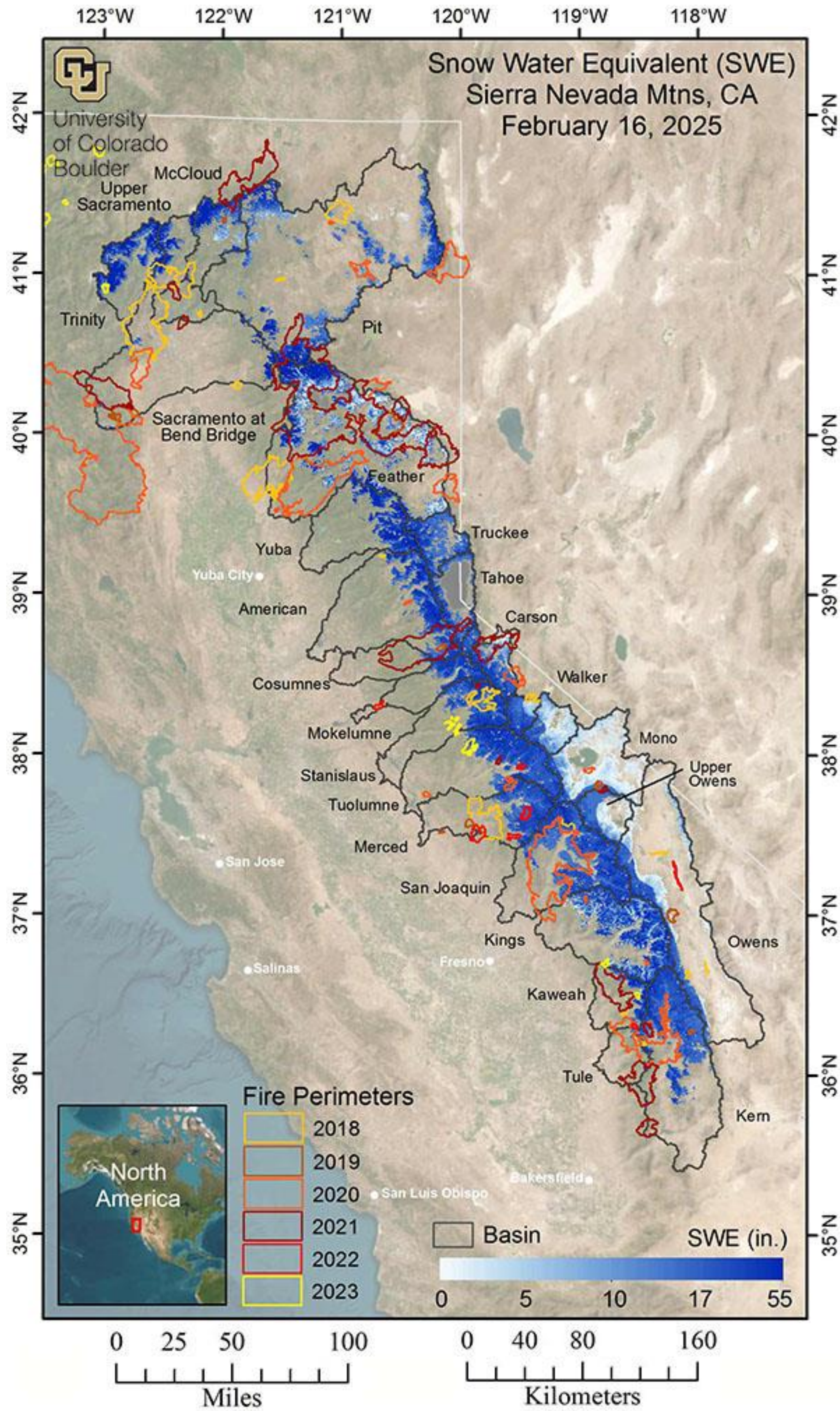

Figure 4. Estimated SWE with Fire Perimeters, Sierra Nevada. SWE amounts are shown with fire perimeters from 2018-2024 (colored from yellow to red).

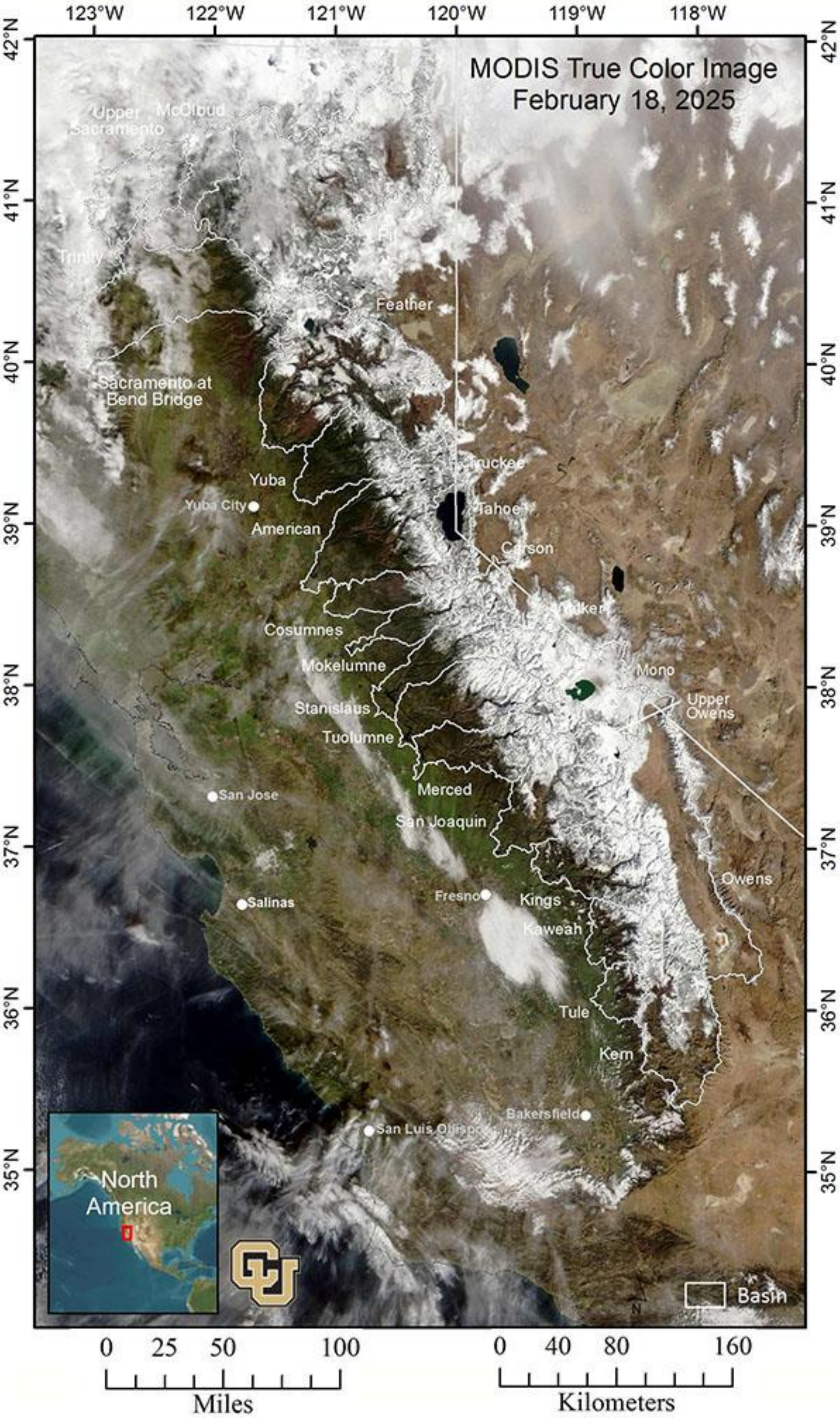

Figure 5. MODIS image, Sierra Nevada. The most recent cloud-free true color MODIS image, showing the Sierra Nevada as close to the model run as possible. Model input fractional snow-covered area (fSCA) was derived from the MODIS Snow Today product (Rittger, et al. 2019) which was calculated using the SPIRES algorithm (Bair, et al. 2021) and from the MODIS cloud-gap-filled product (Hall, et al. 2019).

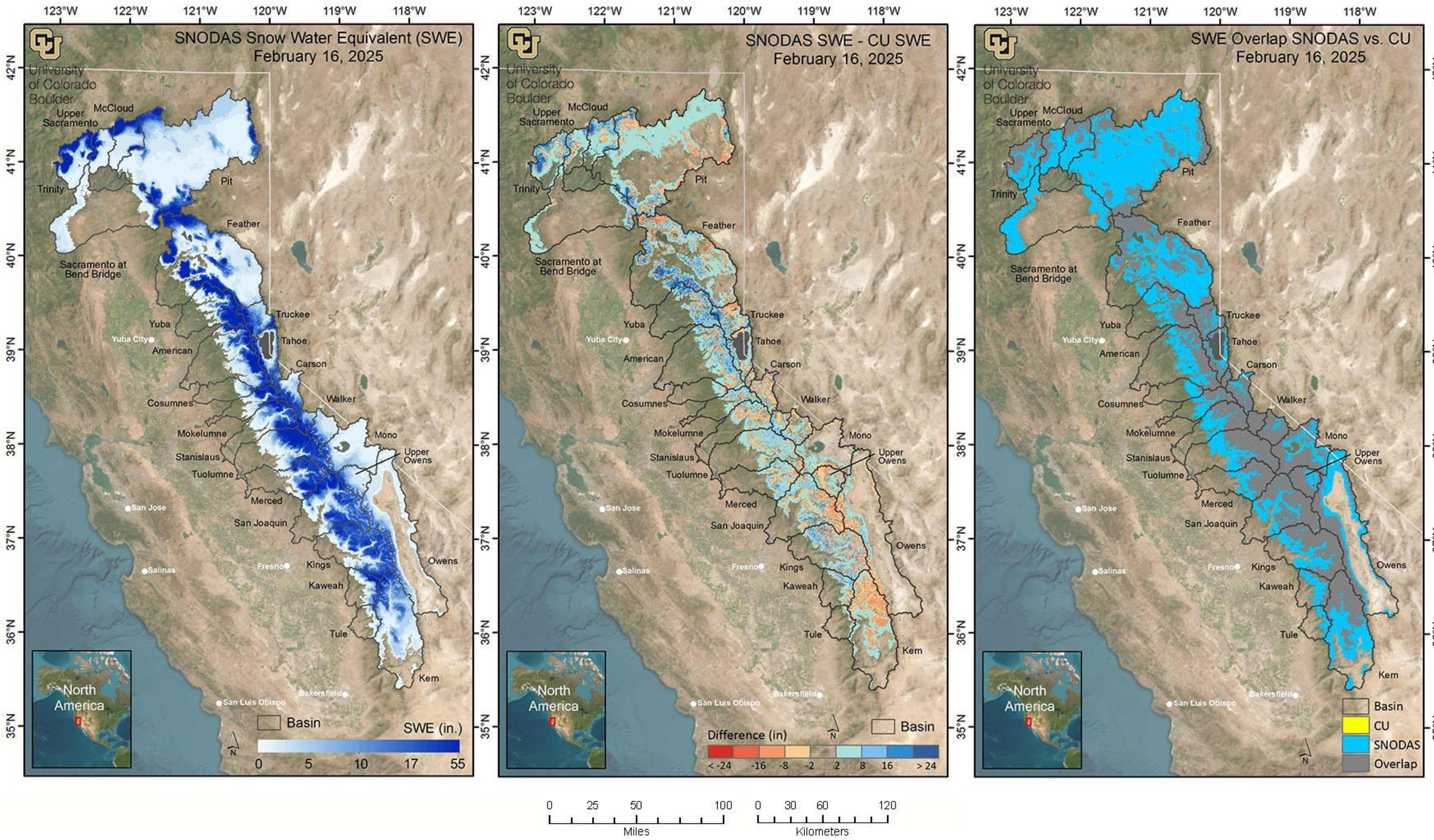

Figure 6. Comparison of CU regression SWE product and SNODAS SWE for the Sierra Nevada. The map on the left shows estimated SWE from the NOAA National Weather Service's National Operational Hydrologic Remote Sensing Center (NOHRSC) SNOw Data Assimilation System (SNODAS). The middle map shows the difference between the SNODAS SWE estimate and CU SWE-fusion estimate. Red pixels denote areas where SNODAS SWE is less than CU SWE and blue pixels show areas where SNODAS SWE is higher than CU SWE. The map on the right shows the snow-cover extent of SNODAS and CU SWE estimates. Yellow pixels show where the location of CU snow extends beyond the location of the SNODAS snow extent. Blue pixels show where the SNODAS snow extends beyond the CU snow extent. Gray areas indicate regions where both products agree on the snow-cover extent.

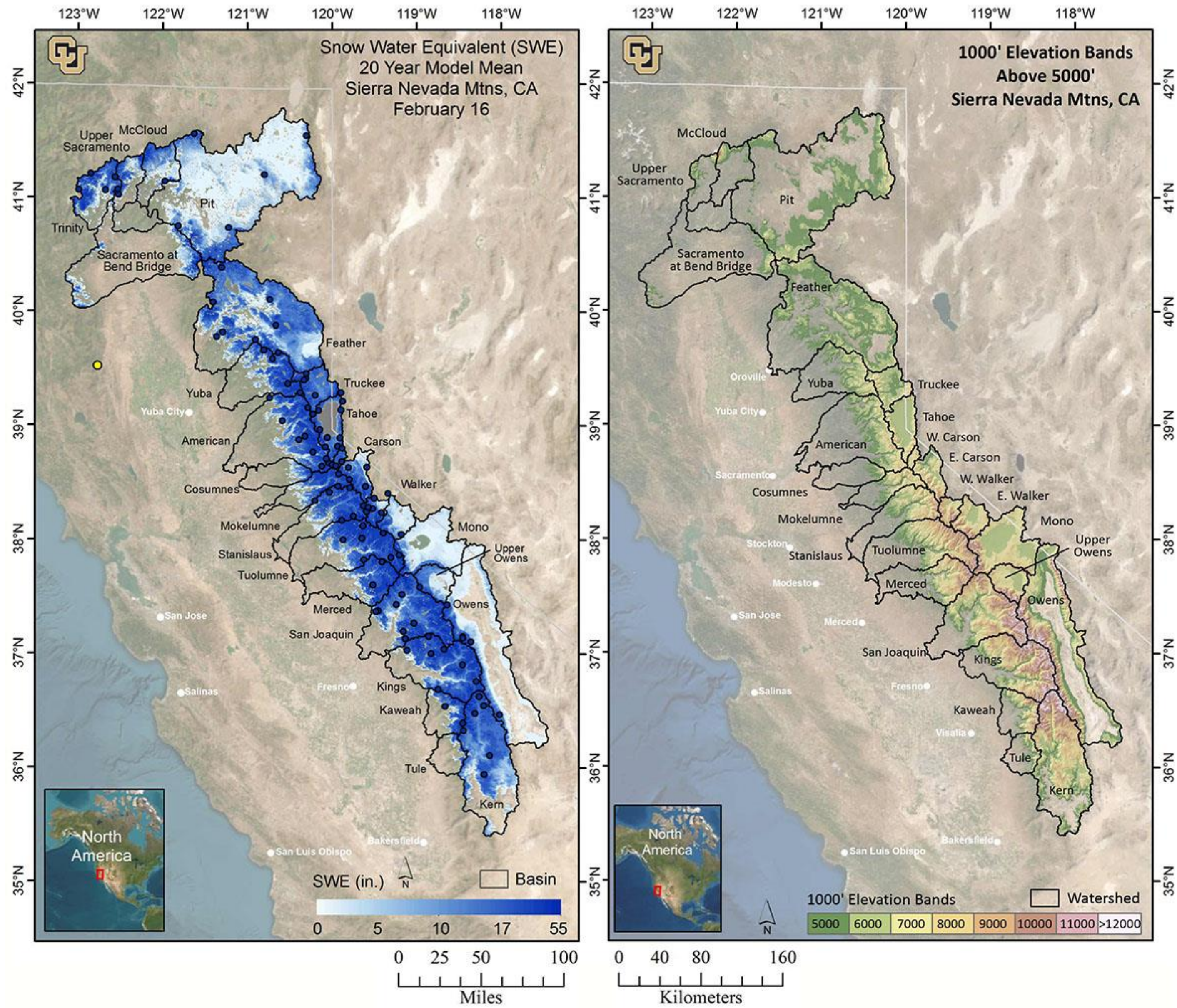

Figure 7. Historical average CU SWE and Elevation Bands for the Sierra Nevada. Long-term (2001-2021) average CU SWE (left), and the Banded Elevation map (right) identifies basins used in this report (black boundaries) and 1000' elevation bands (colored shading) that match those used in Table 1 and Table 2. Map on left shows snow pillow sensor sites recording SWE (black), sites that were offline are shown in red, and sites recording zero are shown in yellow. CoCoRaHS observations if applicable are shown in green.

Methods

The spatial SWE-fusion estimation method is described in Yang, et al. (2022) and Schneider and Molotch (2016). The method uses linear regression in which the dependent variable is derived from the operationally measured in situ SWE from all online snow pillow sensor sites in the domain. The snow pillow sensor SWE observations are scaled by the fractional snow-covered area (fSCA) across the 500 m pixel containing that snow pillow sensor site before being used in the linear regression model. The fSCA is a combination of a near-real-time gap-filled and cloud-free MODIS satellite image which has been processed using the Snow Today algorithm (Rittger, et al. 2019, https://nsidc.org/snow-today), the SPIReS algorithm (Bair, et al. 2021), and the MODIS cloud-gap-filled algorithm (Hall, et al. 2019).

The following independent variables (predictors) enter into the linear regression model:

- Physiographic variables that affect snow accumulation, melt, and redistribution, including elevation, latitude, upwind mountain barriers, slope, and others. See Table 1 in Yang, et al. (2022) for the full set of these variables.
- The historical daily SWE pattern (1985-2021) retrospectively generated using historical MODSCAG data, and an energy-balance model that back-calculates SWE given the fractional Snow-Covered Area (fSCA) time series and meltout date for

each pixel. See Fang, et al. (2022) for details. (For computational efficiency, only one image during the 1985-2021 period that best matches the real-time snow pillow-observed pattern is selected as an independent variable.)

The real-time regression SWE-fusion model for this date has been validated by cross-validation, whereby 10% of the snow pillow data are randomly removed and the model prediction is compared to the measured value at the removed snow pillow stations. This is repeated 12 times to obtain an average R-squared value, which denotes how closely the model fits the snow pillow data. During development of this regression method, the model was also validated against independent historical SWE data collected in snow surveys at 9 locations in Colorado, and an intensive field survey in north-central Colorado. Data utilized to generate this report change to optimize model performance. To maintain consistency across the historical record, the percent of average values are based on our baseline algorithm and therefore there can be discrepancies between absolute SWE values and corresponding percent of averages.

List of All Known Data Issues/Caveats – any of these could apply to this model run

- NEW AVERAGE CALCULATIONS – Average calculations are based on 2001-2021 model values, this includes the drought years (2012-2016) which brings our overall average SWE down considerably, thereby increasing percent of averages.
- RECENT SNOWFALL – There are occasionally problems with lower-elevation SWE estimates due to recent snowfall events that result in extensive snow-cover extending to valley locations where measurements are not available. This scenario results in an over-estimation of lower- elevation SWE.
- LIMITED SNOW PILLOW DATA – When snow at the snow pillow sites melts out, but remains at higher elevations, the model tends to underestimate SWE at the under-monitored upper elevations. This issue typically occurs late in the melt season, resulting in less accurate SWE prediction at higher elevations compared to earlier in the snow season.
- CLOUD COVER – Cloud cover can obscure satellite measurements of snow-cover. While careful checks are made, occasionally the misclassification of clouds as snow or *vice versa* may result in the mischaracterization of SWE or bare-ground.
- LOW LOOK ANGLE – When a satellite does not pass directly over a region but the area is still included within the satellite sensor's field of view, this is referred to as a low "look angle". The resulting image has lower effective resolution – this "blurry" MODSCAG data still contains useful information but may lead to overestimation of SWE near the margins of the snow-cover extent.
- POOR QUALITY SNOW SENSOR DATA – Although data QA/QC is performed, occasional sensor malfunction may result in localized SWE errors.
- ANOMALOUS SNOW PATTERNS – Anomalous snow years or snow distributions may cause SWE error due to the model design to search for similar SWE distributions from previous years. If no close seasonal analogue exists, the model is forced to find the most similar year, which may result in error.
- DENSE FOREST COVER – Dense forest cover at lower elevations where snow-cover is discontinuous can cause the satellite to underestimate the snow-cover extent, leading to underestimation of SWE.
- MISSING SWE VALUES - Data omitted due to inconsistencies with independent SWE estimates.
- PERCENT OF AVERAGE CALCULATIONS - Data utilized to generate this report change to optimize model performance. To maintain consistency across the historical record, the percent of average values are based on our baseline algorithm and therefore there can be discrepancies between absolute SWE values and corresponding percent of averages.
- MODELING METHODS - We work to generate the best SWE estimates for each reporting date. Our methods can change from one report to another. Sometimes data changes between reports is an artifact of method changes.

Table 1. Estimated SWE by basin. *The basin-wide SWE values and averages, are across all pixels at elevations >5000'. Shown are percent of current average SWE (between 2001-2021 as derived from the regression model), mean SWE, percent of snow-covered area, water volume (acre-feet), the area (mi^2) inside each basin that contains data pixels (not including cloud-covered pixels, lakes or other satellite no data pixels), survey data, and snow pillow data, for those areas collected, summarized for each basin. The last column shows mean SWE by basin from SNODAS*.*

Basin	2/1/2025 % 2/1 Avg.	2/16/2025 % 2/16 Avg.	2/1/2025 SWE (in)	2/16/2025 SWE (in)	2/16/2025 % SCA	2/16/2025‡ Vol (af)	Area (mi2) >5000'	2/1/2025 Pillows	2/16/2025 Pillows	2/16/2025 SNODAS*(in)
Trinity	108	127	14.9	22.6	86.3	387,795	321.4	22.1 (4)	28.7 (4)	34
Upper Sacramento	95	136	12.4	22.5	78.7	137,992	115.2	21.3 (2)	33.7 (1)	29.3
McCloud	96	138	10.8	20.1	78.8	176,704	164.9	18.3 (1)	28.5 (1)	33
Pit	60	99	3.2	6.8	36	745,023	2064.7	13.0 (7)	21.3 (7)	8.4
Sacramento at Bend Bridge	36	60	3	7.5	26.9	95,481	239.6	NA	NA	12.2
Feather §	51	77	4.9	9.2	52	1,023,178	2086.6	17.6 (5)	23.7 (6)	12.2
Yuba	65	88	7.8	14.3	60.4	393,708	516.6	25.0 (5)	38.0 (5)	22.8
American	56	69	6.8	11.4	54.3	481,081	792.5	11.4 (10)	17.9 (10)	15.4
Cosumnes	20	25	1.6	2.9	16.7	14,126	91.9	NA	NA	5.7
Mokelumne	56	71	6.7	11.7	57.9	196,500	314.6	14.6 (3)	20.2 (3)	14.6
Stanislaus	55	75	6.3	12.4	65.3	367,879	557.3	12.1 (5)	23.5 (5)	13.2
Tuolumne	57	76	6.8	12.8	65.9	619,433	910	11.1 (7)	20.3 (7)	14.9
Merced	54	79	5.9	12.3	59.7	353,394	538.8	11.6 (2)	22.0 (2)	14.3
San Joaquin	52	81	6.1	13	67.2	838,534	1208.6	5.2 (7)	11.9 (7)	12.8
Kings §	46	80	5.6	12.7	62.9	818,627	1207.5	8.8 (6)	14.4 (7)	13.1
Kaweah	35	62	2.6	7.5	35.6	126,380	314.2	NA	13.7 (2)	9.7
Tule	18	35	0.7	2.1	11.2	15,635	137.6	NA	NA	3.2
Kern	27	66	2.2	7.6	40.9	683,893	1682.1	6.0 (5)	11.7 (6)	5.9
Truckee	56	83	5.8	13.1	71.8	287,332	412	10.6 (6)	17.9 (6)	15.8
Tahoe	55	72	6.3	11.5	63.9	188,194	307	10.0 (7)	18.4 (7)	13.5
W Carson	73	95	8.9	16.2	86.4	55,582	64.3	10.2 (3)	18.3 (3)	16.3
E Carson	61	91	5.3	11.5	73.5	216,411	354.3	8.9 (3)	12.3 (4)	10.6
W Walker	74	101	8.2	15	97.3	143,443	179.6	11.5 (3)	18.2 (4)	16.8
E Walker	63	99	3.2	7.3	85.7	137,233	351.1	6.2 (1)	12.6 (1)	8
Mono	40	82	1.4	3.7	67.9	200,733	1004.9	NA	NA	3.9
Upper Owens	46	89	2.9	8	74	160,452	374.6	12.8 (1)	27.3 (1)	6.9
Owens	37	86	1.3	3.8	37.5	361,150	1772.2	6.5 (4)	11.9 (5)	3.1

§ Data in all ASO-collected basins have been bias-corrected using ASO data and therefore the SWE changes might not represent snowmelt/accumulation but rather an update to the SWE estimates based on airborne data.

‡ For volume totals above Shasta Lake add Upper Sac, McCloud and Pit volumes. For volume totals above Bend Bridge add Upper Sac, McCloud, Pit and Sac at Bend Bridge volumes.

* This is a comparison to the SNODAS (SNOw Data Assimilation System) nationwide product from the National Weather Service.

† Deep and recent snow in areas that typically are snow-free can report high percent of average for this date because the mean 2001-2021 regression-derived SWE for that area is low or 0.

- Data omitted due to inconsistencies with independent SWE estimates.

Table 2. Estimated SWE by basin and elevation band. *The basin-wide SWE values and averages, are across all pixels at elevations >5000'. Elevation bands begin at 5000' and extend past the highest point in the basin. Note that the area of the highest 2-5 bands is typically much smaller than the lower bands. Shown are percent of current average SWE (between 2001-2021 as derived from the regression model), mean SWE, percent of snow-covered area, water volume (acre-feet), the area (mi^2) inside each basin that contains data pixels (not including cloud-covered pixels, lakes or other satellite no data pixels), survey data, and snow pillow data, for those areas collected, summarized for each 1000' elevation band inside each basin. The last column shows mean SWE from SNODAS*.*

Basin	Elevation Band	2/1/2025 % 2/1 Avg.	2/16/2025 % 2/16 Avg.	2/1/2025 SWE (in)	2/16/2025 SWE (in)	2/16/2025 % SCA	2/16/2025 Vol (af)‡	Area (mi2) >5,000'	2/1/2025 Pillows	2/16/2025 Pillows	2/16/2025 SNODAS* (in)
Trinity	5000 - 6000'	108	115	12.1	17.9	80.1	145,255	152.3	18.5 (2)	24.7 (2)	26.2
	6000-7000'	110	138	17.1	26.2	91.4	186,039	133	25.7 (2)	32.7 (2)	39.7
	7000-8000'	102	131	18.9	29.3	93.9	54,844	35.1	NA	NA	46.4
	>8,000'	101	125	17.3	32.2	85.1	1,655	1	NA	NA	46.9
Upper Sacramento	5000 - 6000'	89	125	9.8	18.2	71.8	62,235	64.1	23.6 (1)	33.7 (1)	22.5
	6000-7000'	102	142	14.8	25.5	86.2	49,163	36.2	19.0 (1)	NA	35.1
	7000-8000'	101	135	16.7	27.4	90.1	12,839	8.8	NA	NA	39.6
	8000-9000'	98	140	16.9	27.8	90	3,437	2.3	NA	NA	48.3
	9000-10,000'	86	117	19.3	29.3	88.1	2,718	1.7	NA	NA	57.3
	10,000-11,000	81	199	20.2	54.7	87.9	2,532	0.9	NA	NA	54
	>11,000'	89	278	24	82	90.9	5,065	1.2	NA	NA	49.7
McCloud	5000 - 6000'	94	133	8.3	15.5	71.3	80,180	96.8	18.3 (1)	28.5 (1)	25.6
	6000-7000'	99	143	12.7	24.2	85.9	53,811	41.7	NA	NA	36.1
	7000-8000'	94	138	14.8	26.8	92.9	20,258	14.2	NA	NA	48
	8000-9000'	98	124	16.8	24.3	93.4	8,388	6.5	NA	NA	60.7
	9000-10,000'	95	130	19.5	30.7	99.4	5,056	3.1	NA	NA	59.1
	10,000-11,000	91	167	21.5	45.7	99.3	3,531	1.4	NA	NA	64.2
	>11,000'	109	244	27.1	88.7	96.8	5,478	1.2	NA	NA	56.4
Pit	5000 - 6000'	31	68	1.1	3.2	20.3	243,235	1411.1	26.7 (1)	38.0 (1)	5.5
	6000-7000'	82	123	6.2	12.7	66.3	341,714	502.8	12.6 (3)	20.3 (3)	12.3
	7000-8000'	103	135	11.8	19.2	80.8	132,752	129.4	8.9 (3)	16.6 (3)	22.7
	8000-9000'	115	146	16.1	24	88.3	24,804	19.4	NA	NA	24.7
	>9,000'	105	125	17.6	24.4	86.2	2,516	1.9	NA	NA	33.1
Sacramento at Bend Bridge	5000 - 6000'	12	26	0.7	2.6	12.1	21,564	155.9	NA	NA	7.9
	6000-7000'	50	81	5.2	12.5	44.9	42,209	63.1	NA	NA	16.8
	7000-8000'	83	130	13.1	27.7	82.6	23,137	15.6	NA	NA	28.4
	8000-9000'	83	132	16.7	33.1	87.7	7,661	4.3	NA	NA	39.9
	>9,000'	85	117	17.8	29.4	89.2	907	0.6	NA	NA	53.7
Feather §	5000 - 6000'	38	60	3.1	5.5	39.1	358,386	1229.4	19.2 (1)	24.6 (1)	9.7
	6000-7000'	61	90	6.8	12.9	67.3	503,149	729.8	17.2 (4)	25.5 (4)	14.7
	7000-8000'	81	111	10.8	23.5	88.2	153,707	122.5	NA	15.8 (1)	22.1
	>8,000'	83	108	14.7	30.8	95.7	7,935	4.8	NA	NA	27.9
Yuba	5000 - 6000'	26	36	1.9	4.3	22	43,367	190.8	NA	NA	13.1
	6000-7000'	75	102	10	18.2	78.4	202,328	207.9	23.9 (4)	35.0 (4)	25.1
	7000-8000'	85	115	13.5	23.4	90.7	140,696	112.5	29.5 (1)	50.3 (1)	33.8
	>8,000'	86	114	16.2	25.8	95.3	7,314	5.3	NA	NA	46.1
American	5000 - 6000'	14	17	1	2.1	11.1	32,862	288.8	7.3 (3)	8.5 (3)	6.7
	6000-7000'	62	75	7.4	12.9	66.1	182,031	264	15.8 (1)	22.0 (1)	14.9
	7000-8000'	82	103	12.7	20.3	92.4	178,930	165	13.8 (4)	19.8 (4)	25.3
	8000-9000'	82	103	13.8	21.8	95.7	78,280	67.3	10.4 (2)	26.4 (2)	29.4
	>9,000'	78	98	14.2	22.6	95.9	8,976	7.4	NA	NA	28.1
Cosumnes	5000 - 6000'	0	1	0	0.1	0.5	278	60.5	NA	NA	3.5
	6000-7000'	27	37	2.8	5.9	37.8	7,518	23.7	NA	NA	8.1
	>7,000'	72	81	10.4	15.6	79.6	6,329	7.6	NA	NA	16.2
Mokelumne	5000 - 6000'	2	4	0.1	0.4	2.5	1,641	80.7	NA	NA	1.8
	6000-7000'	27	39	2.2	6	36.9	20,285	63.1	3.5 (1)	8.3 (1)	7.4
	7000-8000'	74	93	9.9	17.4	87.2	79,936	86.2	NA	NA	20.7
	8000-9000'	81	102	13.2	20.9	96.5	85,820	77	20.1 (2)	26.2 (2)	26.1
	>9,000	80	102	13.5	22	96.3	8,816	7.5	NA	NA	25.2
Stanislaus	5000 - 6000'	0	6	0	0.6	3.5	3,336	105.2	NA	NA	1.6
	6000-7000'	28	49	2.1	7.4	47.3	50,659	129.2	NA	NA	6.9
	7000-8000'	65	88	7.3	15.6	87.3	119,201	143.3	12.0 (2)	23.3 (2)	16.1
	8000-9000'	78	100	11.4	19.7	96.7	121,292	115.4	13.1 (2)	24.0 (2)	22.8
	9000-10,000'	79	98	13.3	21.1	96.6	58,152	51.6	10.2 (1)	22.8 (1)	22.5
	10,000-11,000	76	98	14	22.8	97.9	14,775	12.2	NA	NA	19.9
	>11,000'	69	101	11.6	22.4	99.5	460	0.4	NA	NA	12.5

Basin	Elevation Band	2/1/2025 % 2/1 Avg.	2/16/2025 % 2/16 Avg.	2/1/2025 SWE (in)	2/16/2025 SWE (in)	2/16/2025 % SCA	2/16/2025 Vol (af)‡	Area (mi2) >5,000'	2/1/2025 Pillows	2/16/2025 Pillows	2/16/2025 SNODAS* (in)
Tuolumne	5000 - 6000'	0	1	0	0.1	0.3	469	166.9	NA	NA	1.9
	6000-7000'	15	33	1	4.7	29.7	35,220	140.6	0.5 (1)	9.9 (1)	6.3
	7000-8000'	61	84	6.2	14.8	83.5	117,021	148.6	15.6 (1)	23.2 (1)	15.9
	8000-9000'	73	99	9.8	19.1	95.2	169,258	166.4	11.8 (3)	21.0 (3)	22.9
	9000-10,000'	75	94	11.6	19.1	95.5	178,161	174.9	13.2 (2)	23.0 (2)	23.7
	10,000-11,000	75	91	13.1	19.7	95.8	90,886	86.3	NA	NA	20
	11,000-12,000	68	90	12.4	20.1	95.9	25,554	23.8	NA	NA	10.8
	>12,000'	59	98	10.5	22.2	97.1	2,859	2.4	NA	NA	6.6
Merced	5000 - 6000'	0	3	0	0.1	0.5	400	69.7	NA	NA	1.4
	6000-7000'	10	24	0.6	2.8	15.6	11,802	78.3	NA	NA	5
	7000-8000'	48	78	4.5	12.5	67.8	88,154	131.9	NA	NA	13.6
	8000-9000'	64	94	7.7	16.7	80.4	109.562	122.8	11.6 (2)	22.0 (2)	22.1
	9000-10,000'	71	92	11	18.5	86.2	82,999	84.1	NA	NA	22
	10,000-11,000	71	93	12.6	20.5	92.5	43,476	39.7	NA	NA	18
	11,000-12,000	69	97	13.9	24.4	96.1	14,434	11.1	NA	NA	10.7
	>12,000'	65	127	15.3	35.6	99.2	2,564	1.4	NA	NA	8.6
San Joaquin	5000 - 6000'	0	1	0	0.1	0.6	659	133.5	NA	NA	1.5
	6000-7000'	19	36	1.2	4.5	29.6	41,932	175.6	3.7 (3)	9.0 (3)	5.3
	7000-8000'	48	80	4.6	11.7	73.5	130,487	208.7	4.3 (3)	11.2 (3)	11.5
	8000-9000'	53	93	5.8	15.1	79.8	156,261	194.2	NA	NA	19.2
	9000-10,000'	62	94	8.4	17.4	85.5	186,044	200.8	12.6 (1)	23.1 (1)	20.5
	10,000-11,000	69	96	11.5	19.6	93.2	163,287	155.9	NA	NA	16.3
	11,000-12,000	64	96	11.7	20.9	95.9	125,222	112.5	NA	NA	12
	12,000-13,000	61	103	11	23.9	95.7	33,179	26.1	NA	NA	8.7
	>13,000'	52	86	8.1	18.9	90.3	1,459	1.4	NA	NA	7
Kings §	5000 - 6000'	0	1	0	0.1	0.3	264	95.3	NA	NA	1.2
	6000-7000'	2	6	0.1	0.4	4.2	2,998	127.5	NA	5.0 (1)	3.3
	7000-8000'	20	42	1.4	4.4	33.9	39,087	168.1	1.5 (1)	2.9 (1)	8.6
	8000-9000'	41	82	4.1	14	68.3	156,924	210.1	8.1 (1)	15.8 (1)	15.8
	9000-10,000'	57	96	7.3	18.8	84.1	216,827	216.8	13.8 (1)	21.5 (1)	18.7
	10,000-11,000	63	103	10	18.9	94.2	197,054	195.4	9.7 (3)	18.5 (3)	18.8
	11,000-12,000	61	99	10.8	19.2	96.6	150,547	147.4	NA	NA	15.4
	12,000-13,000	56	96	10.4	21.6	94.1	50,919	44.1	NA	NA	12.2
	>13,000'	48	97	9.2	26.8	92.4	4,003	2.8	NA	NA	9.8
Kaweah	5000 - 6000'	0	0	0	0	0	0	55.5	NA	NA	0.8
	6000-7000'	0	0	0	0	0.1	80	59.5	NA	3.6 (1)	2.5
	7000-8000'	9	20	0.5	2.6	15.3	8.325	60.1	NA	NA	7.3
	8000-9000'	31	61	2.2	10	54.1	30,259	56.8	NA	NA	12.8
	9000-10,000'	52	91	6.1	17.4	79.6	40,420	43.4	NA	23.9 (1)	19.4
	10,000-11,000	63	107	10.1	22.7	96.2	35,890	29.6	NA	NA	22
	>11,000'	58	102	9.9	23.1	97.5	11,405	9.3	NA	NA	19.7
Tule	5000 - 6000'	0	0	0	0	0	0	51.6	NA	NA	0.4
	6000-7000'	0	0	0	0	0	0	40	NA	NA	1.9
	7000-8000'	11	19	0.8	2.4	13.5	3,401	26.8	NA	NA	5.4
	8000-9000'	28	63	3.4	10.6	57.9	8,582	15.2	NA	NA	9
	>9,000'	48	87	6.8	16.9	76.3	3,652	4.1	NA	NA	14.4
Kern	5000 - 6000'	0	1	0	0	0.1	264	246.2	NA	NA	0.5
	6000-7000'	0	4	0	0.3	1.8	5,473	341.5	NA	NA	1.6
	7000-8000'	4	23	0.3	2.6	15.3	45,918	326.6	0.8 (1)	4.8 (1)	4
	8000-9000'	24	83	2	12.1	69.9	202,444	314.7	NA	NA	6.6
	9000-10,000'	43	102	4.2	16	87.5	161,768	189.2	9.7 (1)	10.4 (2)	11
	10,000-11,000	55	105	7.1	18.2	90.9	125,588	129.2	6.4 (2)	12.5 (2)	14.3
	11,000-12,000	59	103	9.5	19.8	95.5	96,089	91	6.7 (1)	19.7 (1)	15.7
	12,000-13,000	56	97	9.3	20	95	40,113	37.6	NA	NA	12.6
	>13,000'	47	91	7.9	19.8	95.1	6,232	5.9	NA	NA	8.8

Basin	Elevation Band	2/1/2025 % 2/1 Avg.	2/16/2025 % 2/16 Avg.	2/1/2025 SWE (in)	2/16/2025 SWE (in)	2/16/2025 % SCA	2/16/2025 Vol (af)‡	Area (mi2) >5,000'	2/1/2025 Pillows	2/16/2025 Pillows	2/16/2025 SNODAS* (in)
Truckee	5000 - 6000'	29	66	1.5	8.3	58.6	25,839	58.7	NA	NA	9.4
	6000-7000'	48	78	4.1	11.4	67.2	123,726	203.2	9.1 (4)	15.5 (4)	11.7
	7000-8000'	70	94	9	16.7	80.5	99,270	111.7	13.5 (2)	22.7 (2)	22.7
	8000-9000'	76	97	11.5	19.2	92.7	31,277	30.5	NA	NA	31
	9000-10,000'	75	84	11.3	17	88.1	6,743	7.4	NA	NA	25.3
	10,000-11,000'	77	89	10.7	18.4	100	474	0.5	NA	NA	23.6
Tahoe	6000-7000'	29	49	2.2	6.3	41.4	37,906	113.6	7.7 (2)	13.7 (2)	6.6
	7000-8000'	59	74	7	12.3	69.3	69,089	105.3	11.6 (4)	21.4 (4)	17.1
	8000-9000'	74	90	10.2	16.9	85.1	63,468	70.6	8.4 (1)	15.9 (1)	20.7
	9000-10,000'	77	93	11.9	19	92.9	16,715	16.5	NA	NA	20.7
	>10,000'	68	91	10.8	17.9	97.6	1,014	1.1	NA	NA	15.3
W Carson	5000 - 6000'	0	41	0	4.3	29.7	65	0.3	NA	NA	6.3
	6000-7000'	11	50	0.3	6.5	37.7	667	1.9	NA	NA	7.1
	7000-8000'	70	96	7.6	15.3	87.4	22,500	27.5	NA	NA	15.9
	8000-9000'	78	96	10.2	17.3	88.3	25,250	27.3	10.2 (3)	18.3 (3)	17
	9000-10,000'	79	95	11.8	18.3	90.4	6,790	6.9	NA	NA	17.7
	>10,000'	63	102	7.4	19.9	100	307	0.3	NA	NA	16.4
E Carson	5000 - 6000'	4	20	0.1	1	4.7	1,660	32.6	NA	NA	1.5
	6000-7000'	22	63	0.9	5.5	46.9	23,227	79.3	NA	1.1 (1)	3.8
	7000-8000'	64	101	4.6	11.6	88	62,142	100.2	7.6 (1)	14.2 (1)	9.2
	8000-9000'	75	102	8.8	16.3	93.9	84,630	97.3	9.5 (2)	16.9 (2)	16.5
	9000-10,000'	74	94	10.9	18.5	94.7	34,148	34.7	NA	NA	19.9
	>10,000'	72	95	11.4	19.4	93.8	10,601	10.2	NA	NA	17.1
W Walker	6000-7000'	41	115	0.8	7.1	98.6	2,794	7.3	NA	NA	6.2
	7000-8000'	65	116	2.7	8.9	99.3	18,326	38.6	4.3 (1)	7.6 (1)	7.5
	8000-9000'	74	107	7	14.1	98	34,789	46.1	8.0 (1)	13.5 (2)	16.1
	9000-10,000'	77	97	11.5	18.1	96.3	58,748	60.7	22.1 (1)	38.2 (1)	22.8
	10,000-11,000	76	95	13.1	20.2	95.5	26,874	24.9	NA	NA	21.1
	>11,000'	64	89	10.5	18.6	90.6	1,910	1.9	NA	NA	15.2
E Walker	6000-7000'	3	60	0	1.4	51.5	4,128	57	NA	NA	3.2
	7000-8000'	35	106	0.7	4.5	87.1	26,375	110.2	NA	NA	4.7
	8000-9000'	66	109	3	8	95.3	37,582	88.1	NA	NA	7.7
	9000-10,000'	77	98	7.3	12.6	96	36,097	53.7	6.2 (1)	12.6 (1)	14.7
	10,000-11,000	76	93	9.6	14.9	94.9	27,625	34.7	NA	NA	16.3
	>11,000'	75	94	8.3	13.9	96.6	5,424	7.3	NA	NA	11.5
Mono	6000-7000'	0	40	0	0.6	45.2	9,401	298.2	NA	NA	1.3
	7000-8000'	10	63	0.2	1.8	66	37,721	389.9	NA	NA	2.6
	8000-9000'	38	96	1.4	5.8	90.3	54,808	178.7	NA	NA	4.9
	9000-10,000'	61	96	5	10.4	92.3	35,354	63.5	NA	NA	10.8
	10,000-11,000	72	93	9.8	15.1	95	37,603	46.8	NA	NA	15.4
	11,000-12,000	73	93	10.5	17.1	94.5	21,586	23.6	NA	NA	10.6
	>12,000'	62	97	9.6	18.8	94.2	4,258	4.2	NA	NA	6.3
Upper Owens	6000-7000'	0	11	0	0.4	22.4	1,233	61.6	NA	NA	2.2
	7000-8000'	32	90	1.1	5.7	76.1	43,997	143.5	NA	NA	4.7
	8000-9000'	49	103	3.7	12	88.5	48,123	75	NA	NA	9.9
	9000-10,000'	60	97	5.5	12.3	91.5	28,704	43.9	12.8 (1)	27.3 (1)	12.8
	10,000-11,000	66	95	7.9	13.7	93.2	23,568	32.1	NA	NA	11.4
	11,000-12,000	70	93	9.1	15.3	96.1	12,652	15.5	NA	NA	7.8
	>12,000'	66	95	7.5	14.1	93.4	2,173	2.9	NA	NA	5.3
Owens	5000 - 6000'	0	0	0	0	0.9	7	421.9	NA	NA	0.2
	6000-7000'	0	13	0	0.1	6.3	2,164	342.5	NA	NA	1
	7000-8000'	1	35	0	0.7	28.8	12,532	314.8	NA	NA	2
	8000-9000'	8	66	0.2	2.6	55.9	24,330	178.7	NA	NA	3.5
	9000-10,000'	27	92	1.5	6.8	78.4	53,627	147.8	5.8 (3)	11.0 (3)	5.9
	10,000-11,000	43	97	3.9	11	88.4	95,908	163.5	8.4 (1)	13.1 (2)	8
	11,000-12,000	54	99	6.7	15.2	92.5	106,543	131.9	NA	NA	8.9
	12,000-13,000	58	103	7.8	17.6	92.4	58,334	62.1	NA	NA	7.2
	>13,000'	53	99	6.5	15.7	88.1	7,700	9.2	NA	NA	5.4

§ Data in all ASO-collected basins have been bias-corrected using ASO data and therefore the SWE changes might not represent snowmelt/accumulation but rather an update to the SWE estimates based on airborne data.

‡ For volume totals above Shasta Lake add Upper Sac, McCloud and Pit volumes. For volume totals above Bend Bridge add Upper Sac, McCloud, Pit and Sac at Bend Bridge volumes.

* This is a comparison to the SNODAS (SNOw Data Assimilation System) nationwide product from the National Weather Service.

- Data omitted due to inconsistencies with independent SWE estimates.

† Deep and recent snow in areas that typically are snow-free can report high percent of average for this date because the mean 2001-2021 regression-derived SWE for that area is low or 0.

Location of Reports and Excel Format Tables

https://github.com/CU-Mountain-Hydrology/SierraNevada

References and Additional Sources

Bair, E.H., T. Stillinger and J. Dozier. (2021). Snow Property Inversion From Remote Sensing (SPIReS): A Generalized Multispectral Unmixing Approach With Examples From MODIS and Landsat 8 OLI. IEEE Transactions on Geoscience and Remote Sensing, 59(9): 7270-7284. DOI: 10.1109/TGRS.2020.3040328.

Fang, Y., Liu, Y. & Margulis, S.A. A western United States snow reanalysis dataset over the Landsat era from water years 1985 to 2021 (2022). Sci Data 9, 677. https://doi.org/10.1038/s41597-022-01768-7.

Hall, D. K., G. A. Riggs, N.E. DiGirolamo and M.O. Román (2019). MODIS Cloud-Gap Filled Snow-Cover Products: Advantages and Uncertainties. *Hydrology and Earth System Sciences*, 23:5227-5241. DOI: 10.5194/hess-23-5227-2019.

Molotch, N.P. (2009). Reconstructing snow water equivalent in the Rio Grande headwaters using remotely sensed snow cover data and a spatially distributed snowmelt model. *Hydrological Processes*, 23. DOI: 10.1002/hyp.7206, 2009.

Molotch, N.P., and S.A. Margulis. (2008). Estimating the distribution of snow water equivalent using remotely sensed snow cover data and a spatially distributed snowmelt model: a multi-resolution, multi-sensor comparison. *Advances in Water Resources*, 31.

Molotch, N.P., and R.C. Bales. (2006). Comparison of ground-based and airborne snow-surface albedo parameterizations in an alpine watershed: impact on snowpack mass balance. *Water Resources Research*, 42, DOI:10.1029/2005WR004522.

Molotch, N.P., and R.C. Bales. (2005). Scaling snow observations from the point to the grid-element: implications for observation network design. *Water Resources Research*, 41. DOI: 10.1029/2005WR004229.

Molotch, N.P., T.H. Painter, R.C. Bales, and J. Dozier. (2004). Incorporating remotely sensed snow albedo into a spatially distributed snowmelt model. *Geophysical Research Letters*, 31. DOI:10.1029/2003GL019063, 2004.

Rittger, K., M. S. Raleigh, J. Dozier, A. F. Hill, J. A. Lutz, and T. H. Painter. 2019. Canopy Adjustment and Improved Cloud Detection for Remotely Sensed Snow Cover Mapping. Water Resources Research 24 August 2019. DOI:10.1029/2019WR024914.

Schneider D. and N.P. Molotch. (2016). Real-time estimation of snow water equivalent in the Upper Colorado River Basin using MODIS-based SWE reconstructions and SNOTEL data. *Water Resources Research*, 52(10): 7892-7910. DOI: 10.1002/2016WR019067.

Yang, K., K. N. Musselman, K. Rittger, S. A. Margulis, T. H. Painter and N. P. Molotch. (2022). Combining ground-based and remotely sensed snow data in a linear regression model for real-time estimation of snow water equivalent. *Advances in Water Resources,* 160, 2022, 104075. DOI: 10.1016/j.advwatres.2021.104075.